Minority-carrier diffusion length, minority-carrier lifetime, and photoresponsivity of β-$FeSi_2$ layers grown by molecular-beam epitaxy

Keiichi Akutsu,[1] Hideki Kawakami,[1] Mitsushi Suzuno,[1] Takashi Yaguchi,[1] Karolin Jiptner,[2] Jun Chen,[2] Takashi Sekiguchi,[2] Teruhisa Ootsuka,[3] and Takashi Suemasu[1,4,a)]
[1]*Institute of Applied Physics, University of Tsukuba, Tsukuba, Ibaraki 305-8573, Japan*
[2]*National Institute for Materials Science, Tsukuba, Ibaraki 305-0044, Japan*
[3]*National Institute of Advanced Industrial Science and Technology, Ibaraki 305-8568, Japan*
[4]*Japan Science and Technology Agency, CREST, Chiyoda-ku, Tokyo 102-0075, Japan*

(Received 15 March 2011; accepted 29 April 2011; published online 17 June 2011)

We have epitaxially grown undoped β-$FeSi_2$ films on Si(111) substrates via atomic-hydrogen-assisted molecular-beam epitaxy. β-$FeSi_2$ films grown without atomic hydrogen exhibited *p*-type conduction with a hole density of over 10^{19} cm^{-3} at room temperature (RT). In contrast, those prepared with atomic hydrogen showed *n*-type conduction and had a residual electron density that was more than two orders of magnitude lower than the hole density of films grown without atomic hydrogen (of the order of 10^{16} cm^{-3} at RT). The minority-carrier diffusion length was estimated to be approximately 16 μm using an electron-beam-induced current technique; this value is twice as large as that for β-$FeSi_2$ prepared without atomic hydrogen. This result could be well explained in terms of the minority-carrier lifetimes measured by a microwave photoconductance decay technique. The 1/*e* decay time using a 904 nm laser pulse was approximately 17 μs, which is much longer than that for β-$FeSi_2$ prepared without atomic hydrogen (3 μs). The photoresponsivity reached 13 mA/W at 1.31 μm, which is the highest value ever reported for β-$FeSi_2$ films. © *2011 American Institute of Physics*. [doi:10.1063/1.3596565]

I. INTRODUCTION

Semiconducting iron disilicide (β-$FeSi_2$) has been attracting considerable interest as a Si-based material operating at optical fiber communication wavelengths. β-$FeSi_2$ has a bandgap of approximately 0.78 eV,[1] and a very high optical absorption coefficient of over 10^5 cm^{-1} at 1 eV.[2] Over the past two decades, there have been numerous reports on the development of infrared light-emitting diodes and detectors using β-$FeSi_2$.[3–8] In particular, a photoresponsivity of over 100 mA/W for 1.31 μm light for *n*-type β-$FeSi_2$ single crystals has renewed interest in this material.[9,10] The photoresponsivity obtained for β-$FeSi_2$ thin films has been increasing each year.[11–14] However, the highest photoresponsivity obtained so far for β-$FeSi_2$ thin films (3.3 mA/W at 1.31 μm)[13] is still more than one order of magnitude smaller than that for *n*-type β-$FeSi_2$ single crystals. This difference is attributed to different minority-carrier diffusion lengths in β-$FeSi_2$. An electron-beam-induced current (EBIC) technique revealed that the minority-carrier diffusion length in single crystalline *n*-type β-$FeSi_2$ is approximately 50 μm.[10] In contrast, the minority-carrier diffusion length of β-$FeSi_2$ films has not been reported. The lower photoresponsivity (and thus shorter minority-carrier diffusion length) in β-$FeSi_2$ films is probably due to defects at the grain boundaries of β-$FeSi_2$ epitaxial variants on Si substrates[15–17] and high residual carrier (hole) concentrations reaching approximately 10^{19} cm^{-3} at room temperature (RT).[18] The grain boundaries of β-$FeSi_2$ are caused mainly by the small difference between lattice constants *b* and *c* of β-$FeSi_2$. In the present study, we attempted to reduce the residual hole concentration.

It is well known that the conduction type of β-$FeSi_2$ depends on the atomic ratio of Si to Fe.[19–22] Tani and Kido performed first-principles calculations of defects in β-$FeSi_2$ using density functional theory. They showed that Si vacancies have lower formation energies than Fe vacancies in β-$FeSi_2$, and that crystals containing Si vacancies exhibit *p*-type conduction.[23] Thus, the high hole concentration in undoped *p*-type β-$FeSi_2$ is considered as due to the presence of Si vacancies. Al doping has been reported to be an effective way to substitute for Si vacancies.[24] However, there have been only a few reports on methods to reduce the residual carrier concentration in β-$FeSi_2$.[25,26] Yoneda *et al.* achieved carrier concentrations of the order of 10^{16} cm^{-3} by precisely controlling the growth conditions in molecular-beam epitaxy (MBE).[25] Shaban *et al.* suggested that introducing atomic hydrogen might be effective for reducing the carrier concentration of $FeSi_2$ films, based on the observation that the resistivity of semiconducting nanocrystalline $FeSi_2$ increased when atomic hydrogen was introduced during sputtering.[26] From an engineering perspective, we consider that atomic hydrogen irradiation is more practical than precisely controlling the MBE growth conditions. However, no experimental data have been reported that demonstrate that atomic hydrogen is effective for reducing the residual carrier concentration of β-$FeSi_2$. In this study, we reduced the carrier concentration by more than two orders of magnitude in undoped β-$FeSi_2$ by using atomic-hydrogen-assisted MBE. The minority-carrier diffusion length and minority-carrier

a)Author to whom correspondence should be addressed. Electronic mail: suemasu@bk.tsukuba.ac.jp.

lifetime were measured in order to confirm this reduction. The photoresponsivity measured at 1.31 μm on a simple Al/*n*-type β-$FeSi_2$ Schottky diode is also discussed.

II. EXPERIMENTAL METHOD

β-$FeSi_2$ films were epitaxially grown via MBE on 500-μm-thick *n*-type floating-zone (FZ) Si(111) ($n \approx 10^{12}$ cm^{-3}) and *n*-type Czochralski (CZ) Si(111) ($n = 7 \times 10^{17}$ cm^{-3}) substrates. The growth procedure employed for β-$FeSi_2$ films is the same as that used previously.[27] Atomic hydrogen was generated by heating a tungsten filament at approximately 1800 °C; the substrate was continuously irradiated with atomic hydrogen during growth. The cracking efficiency of the atomic hydrogen source was approximately 3% at 1800 °C.[28] The beam equivalent pressure of hydrogen P_{H2} was kept constant during growth, but it was varied from sample to sample as follows: 0 Pa (samples A and D), 8×10^{-5} Pa (samples B and E), and 8×10^{-4} Pa (sample C). The samples were prepared as summarized in Table I.

X-ray diffraction (XRD) was used to characterize the crystalline quality of the grown films. Electron backscatter diffraction (EBSD) was performed on samples A–C along the normal direction of the β-$FeSi_2$ films at intervals of 0.1 μm in order to analyze the grain size and preferential orientation of the films. The carrier concentration and mobility were measured at RT on samples A–C, which were the β-$FeSi_2$ films grown on the high-resistivity FZ-Si(111) using the van der Pauw method. The applied magnetic field was 0.54 T normal to the sample surface. Minority carrier diffusion lengths were measured via EBIC technique in the edge-scan configuration with a Hitachi S4300 field-emission scanning electron microscope (SEM) in EBIC mode at RT. The acceleration voltage of the electron beam was 9 kV. For EBIC measurements, Schottky contacts were formed on the β-$FeSi_2$ surfaces of samples D and E via ultrasonic wedge bonding using Al. Ohmic contacts were formed on the front surface of sample D by depositing Au. Ohmic contacts were fabricated on the front and back surfaces of sample E by depositing Al followed by annealing at 450 °C for 20 min in N_2. Minority carrier lifetimes were measured using the microwave photoconductance decay (μ-PCD) method using a light pulse with a wavelength of 904 nm. The photon flux was kept constant at 5×10^{13} photons/cm^2. The photoresponse spectrum of sample E was measured via a lock-in technique using a xenon lamp with a 25-cm-focal-length single monochromator (Bunko Keiki, SM-1700 A). The photogenerated currents were measured in the lateral direction for various bias voltages applied between the Al ohmic contacts (stripes spaced at 1.5 mm on the surface). The light intensity was calibrated using a pyroelectric power meter (Melles Griot, 13PEM001/J). The photoresponsivity of the Al/*n*-β-$FeSi_2$ Schottky diode was measured by irradiating sample E with a 0.78 mW, 1.31 μm laser beam at RT. The spot size of the laser beam was approximately 50 μm, and the emission power was measured using a Ge optical power meter (Newport, 1815-C).

TABLE I. Sample preparation, substrate and growth thicknesses of reactive deposition epitaxy (RDE)- and MBE-grown β-$FeSi_2$ layers, and beam-equivalent pressure P_{H2} during atomic-hydrogen irradiation.

Sample	Substrate	RDE/MBE (nm)	P_{H2} (Pa)
A	FZ-*n*-Si(111)	20/560	—
B	FZ-*n*-Si(111)	20/260	8×10^{-5}
C	FZ-*n*-Si(111)	20/560	8×10^{-4}
D	CZ-n-Si(111)	20/500	—
E	CZ-n-Si(111)	20/630	8×10^{-5}

III. RESULTS AND DISCUSSION

A. Electrical properties

Figures 1(a)–1(c) show θ–2θ XRD patterns of samples A–C, respectively. As shown in Figs. 1(a) and 1(b), peaks from [110]- or [101]-oriented β-$FeSi_2$ are dominant. This orientation of β-$FeSi_2$ relative to the Si(111) surface is consistent with the epitaxial relationship between the two materials.[15] However, on increasing P_{H2}, the [110] or [101] orientation of β-$FeSi_2$ degraded in sample C. Instead, the diffraction peaks of [100]-oriented β-$FeSi_2$ became intense, as shown in Fig. 1(c).

A similar tendency is observed in the EBSD maps shown in Figs. 2(a)–2(c). The mappings indicate that the β-$FeSi_2$(110) (blue) and (101) (yellow) planes in samples A and B are

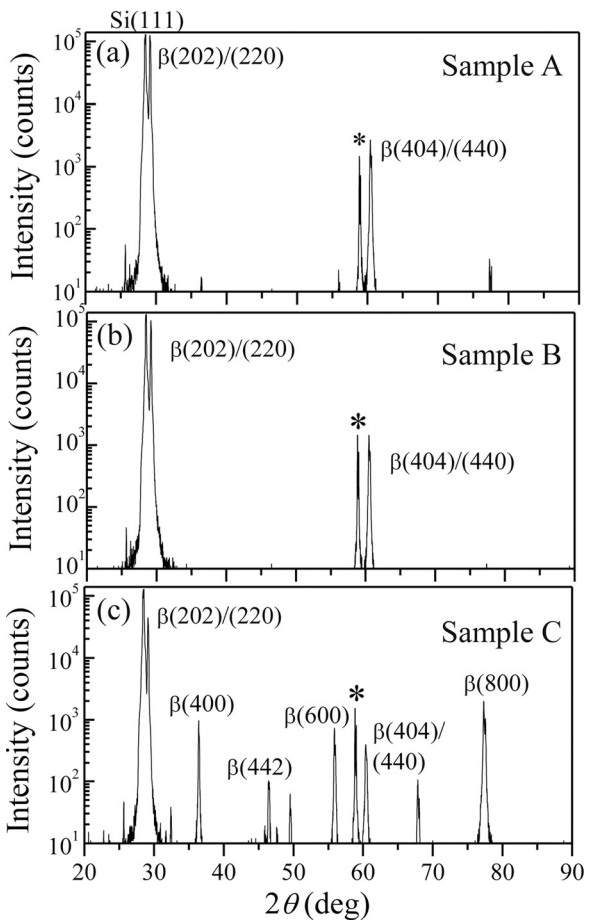

FIG. 1. θ–2θ XRD patterns for (a) sample A, grown without atomic hydrogen, (b) sample B, grown with $P_{H2} = 8 \times 10^{-5}$ Pa, and (c) sample C, grown with $P_{H2} = 8 \times 10^{-4}$ Pa. The forbidden diffraction peak of Si(222) indicated by the asterisk occurs due to double diffraction.

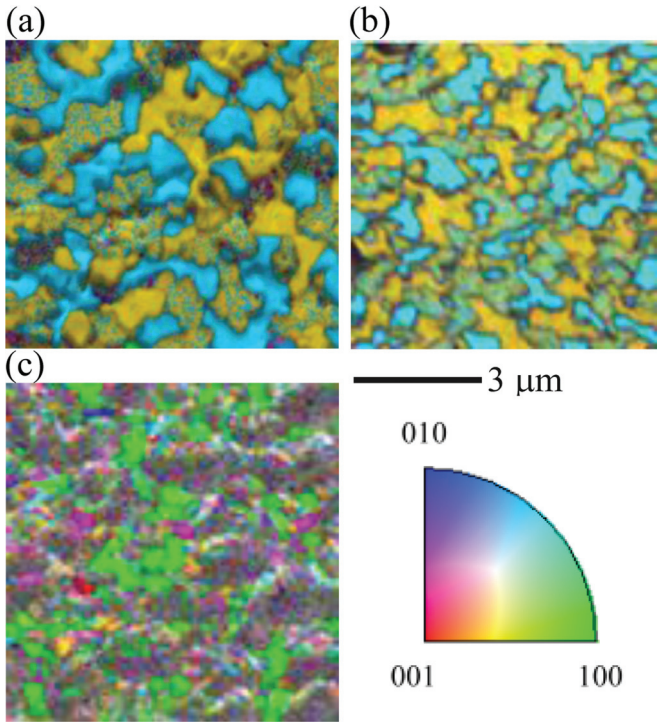

FIG. 2. (Color) EBSD mappings observed along the normal direction for β-$FeSi_2$ in samples (a) A, (b) B, and (c) C.

parallel to the sample surface, but that they are not parallel to the surface in sample C. The grain size can be determined from the areas of regions with the same color. The grain size is roughly estimated to be a few micrometers in sample A, but it decreases with increasing P_{H2}.

Secondary ion mass spectroscopy revealed the presence of hydrogen atoms in samples B and C, as shown in Fig. 3. Even sample A contains hydrogen, probably because of residual hydrogen in the chamber.

Figure 4 shows the measured carrier concentrations and mobilities of samples A–C at RT. We did not observe any nonlinear variation of the Hall voltage with magnetic field.[29] Sample A had a hole concentration p of 3.0×10^{19} cm^{-3} and a hole mobility μ_h of 1.3 $cm^2/V \cdot s$. In contrast, β-$FeSi_2$ grown via atomic-hydrogen-assisted MBE had a much lower carrier concentration and a much higher carrier mobility. The conductivity changed from p- to n-type in sample B, prepared

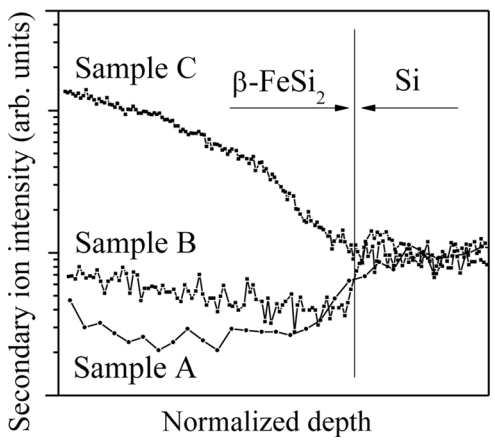

FIG. 3. SIMS depth profiles of hydrogen atoms in samples A–C.

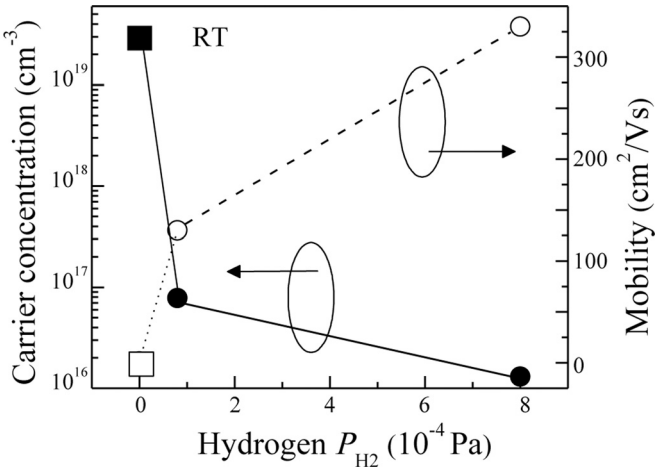

FIG. 4. Dependence of the carrier concentration (■, ●) and mobility (□, ○) in β-$FeSi_2$ films (samples A–C) measured at RT on P_{H2}.

with $P_{H2} = 8 \times 10^{-5}$ Pa, and the residual carrier (electron) concentration n decreased significantly to 7.8×10^{16} cm^{-3}, whereas the electron mobility μ_e increased to 130 $cm^2/V \cdot s$. Furthermore, n decreased (1.3×10^{16} cm^{-3}) and μ_e increased (330 $cm^2/V \cdot s$) in sample C when P_{H2} was further increased from 8×10^{-5} to 8×10^{-4} Pa.

These results imply that β-$FeSi_2$ films grown via atomic-hydrogen-assisted MBE have drastically lower carrier concentrations than do β-$FeSi_2$ films grown without atomic hydrogen, but that excess hydrogen supply degrades the crystalline quality of β-$FeSi_2$. It was difficult to perform reliable Hall measurements on the β-$FeSi_2$ films of samples D and E because of the low resistivity of the Si substrates. However, the β-$FeSi_2$ films in samples D and E are strongly expected to exhibit characteristics similar to those in samples A and B, respectively. We speculate that the reduced carrier densities of samples B and C can be attributed to compensation not by n-type dopants, but by the inactivation of Si vacancies by hydrogen termination or by a reduction in the number of Si vacancies. This is because doping with n-type impurities can change the carrier type from p- to n-type; however, the observed reduction in the carrier density of more than two orders of magnitude is unlikely in this case. Further studies are required in order to determine the exact mechanism for this reduction in the carrier concentration. We consider that positron annihilation lifetime spectroscopy is a powerful technique for evaluating the density of Si vacancies in β-$FeSi_2$.

B. Minority-carrier diffusion length measured via EBIC

We next discuss the minority-carrier diffusion length measurements of β-$FeSi_2$ films via EBIC. Based on the crystalline quality of β-$FeSi_2$, we hereinafter employ the growth conditions for sample B ($P_{H2} = 8 \times 10^{-5}$ Pa) rather than those for sample C ($P_{H2} = 8 \times 10^{-4}$ Pa). For EBIC measurements, we formed a Schottky contact using an Al wire and an ohmic contact on either surface of the β-$FeSi_2$ film, as shown in Fig. 5(a). Figures 5(b), 5(b′), 5(c) and 5(c′) show SEM and EBIC images around the Al contact on β-$FeSi_2$ films grown without atomic hydrogen (sample D) and with atomic hydrogen at $P_{H2} = 8 \times 10^{-5}$ Pa (sample E), respectively. In the

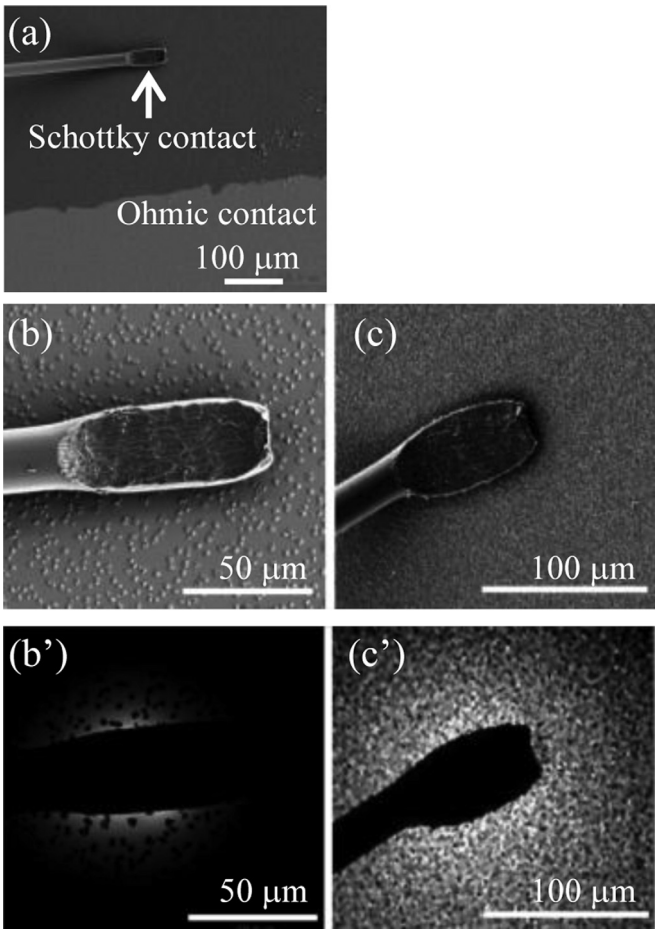

FIG. 5. (a)–(c) SEM and (b′),(c′) EBIC images around the Al contact on β-$FeSi_2$ films in samples (a),(b),(b′) D and (c),(c′) E.

EBIC method, minority carriers generated within the diffusion length in *p*- and *n*-type β-$FeSi_2$ are concentrated by the electric field around the Al contact and detected as a current in the external circuit in samples D and E, respectively. In Figs. 5(b′) and 5(c′), the brighter regions indicate higher concentrations of electron-beam-induced carriers in β-$FeSi_2$. Figure 6 shows semilogarithmic plots of EBIC line-scan profiles of samples D and E. The EBIC profiles show a clear exponential dependence on the distance from the Al contacts. In this study,

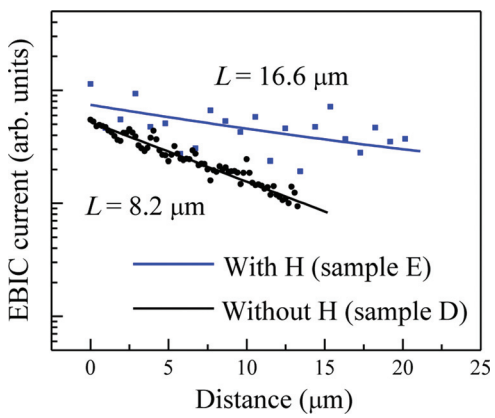

FIG. 6. (Color online) Semilogarithmic plots of EBIC line-scan profiles measured on β-$FeSi_2$ films in samples D and E.

the minority-carrier diffusion lengths were estimated to be approximately 8.2 μm for sample D (grown without atomic hydrogen) and approximately 16.6 μm for sample E (grown with atomic hydrogen at $P_{H2} = 8 \times 10^{-5}$ Pa), assuming that the EBIC profile varies as exp $(-x/L)$, where x is the distance from the Al edge along the line and L is the diffusion length of minority carriers. These results indicate an increased minority-carrier diffusion length in β-$FeSi_2$ in sample E. However, the minority-carrier diffusion length of 16.6 μm in sample E is still much smaller than the 50 μm obtained for the single-crystalline *n*-type β-$FeSi_2$.[10] This is thought to be due to defects at the grain boundaries in the β-$FeSi_2$ films, as shown in Fig. 2.

C. Minority-carrier lifetime using μ-PCD

Next, we measured the minority-carrier lifetimes at RT for the β-$FeSi_2$ layers in samples D and E. Figures 7(a) and 7(b) show the decay curves of reflected light using a 904-nm light pulse. At this wavelength, the absorption coefficient of β-$FeSi_2$ is more than 2×10^5 cm^{-1}.[30] Therefore, most photons are likely to be absorbed in the β-$FeSi_2$ layers. From the decay curves, the $1/e$ decay time was extracted as a measure of the minority-carrier lifetime; that is, 3.2 μs and 17.4 μs for samples D and E, respectively. The diffusion length L is related to the carrier lifetime τ by $L = \sqrt{D\tau}$, where D is the diffusion coefficient. The square root of the ratio of the minority-carrier lifetime $\sqrt{17.4\,\mu s/3.2\,\mu s} \cong 2.3$ is in good quantitative agreement with the ratio of the minority-carrier diffusion length (16.6 μm/8.2 μm) $\cong 2.0$. Therefore, the enhancement of the minority-carrier diffusion length is attributed to the increase in the minority-carrier lifetime caused by the reduction in the residual carrier concentration in β-$FeSi_2$.

D. Photoresponse

We chose sample E for photoresponse measurements. Figure 8 shows the temperature dependence of photoresponse spectra obtained for sample E. Five volts were applied between the striped Al electrodes spaced at 1.5 mm. Light absorption produces electron–hole pairs that are separated by

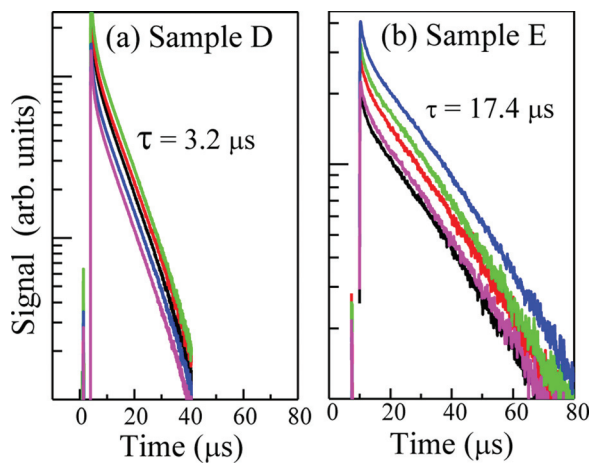

FIG. 7. (Color online) Decay curves of reflected light intensity for β-$FeSi_2$ films measured via μ-PCD in (a) sample D and (b) sample E. Measurements were performed at five different points on each sample.

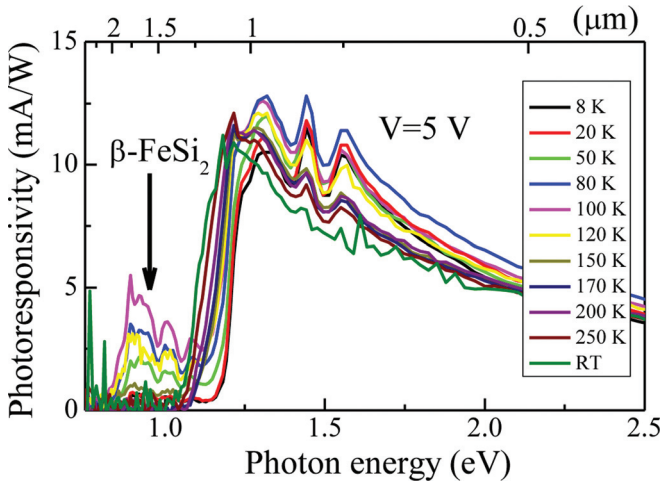

FIG. 8. (Color online) Temperature dependence of photoresponsivity in sample E.

the electric field between the electrodes, leading to current flow in the external circuit as the photoexcited carriers drift before recombining. The photocurrents increased sharply at around 0.78 and 1.1 eV. These energies correspond to the optical absorption edges of β-$FeSi_2$ and Si, respectively. The observed photoresponsivity due to β-$FeSi_2$ reached a maximum at around 100 K, but it became too small to detect at RT. This is because photoexcited carriers drifted in the lateral direction in this measurement, and thus the carriers are likely to experience grain boundaries, as shown in the EBSD mappings of Fig. 2. In contrast, an enhanced photoresponsivity can be strongly expected for carriers traveling in the normal direction as in *pn* or Schottky junctions, because a much larger built-in electric field exists around the junction, and also because the distance that photoexcited carriers must travel is much shorter than that in the present case. Thus, we measured the photoresponsivity in the Al/*n*-β-$FeSi_2$ Schottky diode.

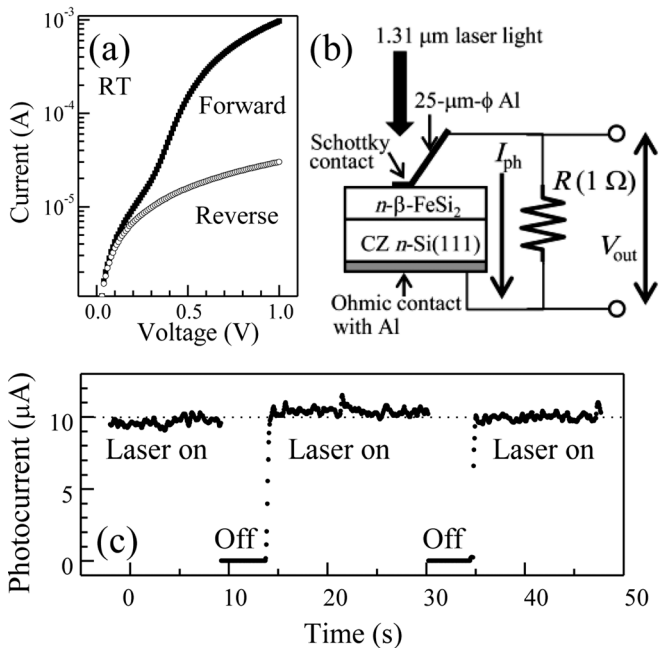

FIG. 9. (a) *I–V* characteristics of the Al/*n*-β-$FeSi_2$ diode in sample E. (b) Schematic setup for the photoresponsivity measurement. (c) Photoresponse of the diode when the 0.78 mW, 1.31 μm laser is on and off.

Figure 9(a) shows the current–voltage (*I–V*) characteristics of the Al/*n*-β-$FeSi_2$ Schottky diode (sample E) under dark conditions. An ohmic contact was formed on the backside with Al. More current flows when a positive bias is applied to the Al wire with respect to the *n*-Si substrate. These results reveal that the Al/*n*-type β-$FeSi_2$ junction forms a Schottky diode even though there are some leakage currents. Figure 9(b) shows the schematic setup for the photoresponse measurement. A 1.31 μm laser light was incident in the same way as reported in Refs. 13 and 14. Upon laser light irradiation, the photoresponsivity reached approximately $(10\,\mu A/0.78\,mW) \cong 13$ mA/W, as shown in Fig. 9(c). This value is the highest value ever reported for β-$FeSi_2$ films. At present, the β-$FeSi_2$ grain size is a few micrometers, which is much smaller than the laser spot size (50 μm) used in optical measurements. Thus, we think that a much higher photoresponsivity can be safely expected in β-$FeSi_2$ films that have much larger grain sizes.

IV. SUMMARY

We have epitaxially grown β-$FeSi_2$ films on Si(111) via MBE using a cracking cell for generating atomic hydrogen. The conduction type changed from *p*- to *n*-type, and the carrier concentration was two orders of magnitude (of an order of $n \approx 10^{16}$ cm^{-3}) lower than that for films grown in the absence of atomic hydrogen. The minority-carrier diffusion length increased from approximately 8 μm to 16 μm, and consequently the minority-carrier lifetime increased by a factor of approximately four. A photoresponsivity of approximately 13 mA/W was obtained at 1.31 μm.

ACKNOWLEDGMENTS

This work was supported in part by a Grant-in-Aid for Scientific Research (2136002) from the Ministry of Education, Culture, Sports, Science and Technology of Japan, and also by JST, CREST.

[1]H. Udono, I. Kikuma, T. Okuno, Y. Masumoto, and H. Tajima, Appl. Phys. Lett. **85**, 1937 (2004).
[2]M. C. Bost and J. E. Mahan, J. Appl. Phys. **58**, 2696 (1985).
[3]K. Lefki and P. Muret, J. Appl. Phys. **74**, 1138 (1993).
[4]D. Leong, M. Harry, K. J. Reeson, and K. P. Homewood, Nature **387**, 686 (1997).
[5]Y. Maeda, T. Akita, K. Umezawa, K. Miyake, and M. Sagawa, Proc. SPIE **3419**, 354 (1998).
[6]T. Suemasu, Y. Negishi, K. Takakura, and F. Hasegawa, Jpn. J. Appl. Phys., Part 2 **39**, L1013 (2000).
[7]M. Suzuno, T. Koizumi, and T. Suemasu, Appl. Phys. Lett. **94**, 213509 (2009).
[8]M. Shaban, K. Nomoto, S. Izumi, and T. Yoshitake, Appl. Phys. Lett. **94**, 222113 (2009).
[9]T. Ootsuka, T. Suemasu, J. Chen, and T. Sekiguchi, Appl. Phys. Lett. **92**, 042117 (2008).
[10]T. Ootsuka, T. Suemasu, J. Chen, T. Sekiguchi, and Y. Hara, Appl. Phys. Lett. **92**, 192114 (2008).
[11]Y. Maeda, K. Umezawa, Y. Hayashi, K. Miyake, and K. Ohashi, Thin Solid Films **381**, 256 (2001).

[12]Z. X. Liu, M. Osamura, T. Ootsuka, S. Wang, Y. Fukuzawa, Y. Suzuki, R. Kuroda, T. Mise, N. Otogawa, Y. Nakayama, H. Tanoue, and Y. Makita, Opt. Mater. **27**, 942 (2005).
[13]M. Shaban, K. Nomoto, S. Izumi, and T. Yoshitake, Appl. Phys. Lett. **94**, 222113 (2009).
[14]M. Shaban, S. Izumi, K. Nomoto, and T. Yoshitake, Appl. Phys. Lett. **95**, 162102 (2009).
[15]K. M. Geib, J. E. Mahan, R. G. Long, M. Nathan, and G. Bai, J. Appl. Phys. **70**, 1730 (1991).
[16]H. U. Nissen, E. Müller, H. R. Deller, and H. V. Känel, Phys. Status Solidi A **150**, 395 (1995).
[17]K. Akiyama, S. Ohya, H. Takano, N. Kieda, and H. Funakubo, Jpn. J. Appl. Phys., Part 2 **40**, L460 (2001).
[18]See, for example, M. Suzuno, Y. Ugajin, S. Murase, and T. Suemasu, J. Appl. Phys. **102**, 103706 (2007).
[19]M. Komabayashi, K. Hijikata, and S. Ido, Jpn. J. Appl. Phys., Part 1 **29**, 1118 (1990).
[20]T. Miki, Y. Matsui, K. Matsubara, and K. Kishimoto, J. Appl. Phys. **75**, 1693 (1994).
[21]T. Miki, Y. Matsui, Y. Teraoka, Y. Ebina, K. Matsubara, and K. Kishimoto, J. Appl. Phys. **76**, 2097 (1994).
[22]K. Takakura, T. Suemasu, Y. Ikura, and F. Hasegawa, Jpn. J. Appl. Phys., Part 2 **39**, L789 (2000).
[23]J. Tani and H. Kido, J. Alloys Compd. **352**, 153 (2003).
[24]Y. Terai and Y. Maeda, Appl. Phys. Lett. **84**, 903 (2004).
[25]K. Yoneda, Y. Terai, K. Noda, N. Miura, and Y. Fujiwara, Ext. Abstr., in *Proceedings of the 71st Fall Meeting*, Japan Society of Applied Physics and Related Societies, 17a-NH-7, Nagasaki, Japan, 14–17 September 2010 [in Japanese].
[26]M. Shaban, H. Kondo, K. Nakashima, and T. Yoshitake, Jpn. J. Appl. Phys., Part 1 **47**, 5420 (2008).
[27]M. Takauji, N. Seki, T. Suemasu, F. Hasegawa, and M. Ichida, J. Appl. Phys. **96**, 2561 (2004).
[28]A. Sutoh, Y. Okada, S. Ohta, and M. Kawabe, Jpn. J. Appl. Phys., Part 2 **34**, L1379 (1995).
[29]H. Lange, Phys. Status Solidi B **201**, 3 (1997).
[30]K. Yamaguchi and H. Udono, Int. J. Hydrogen Energy **32**, 2726 (2007).